RSC Advances

PAPER

View Article Online
View Journal | View Issue

Cite this: *RSC Adv.*, 2017, **7**, 30582

Ultra-selective detection of Fe^{2+} ion by redox mechanism based on fluorescent polymerized dopamine derivatives†

Taeuk An,‡[a] Namhun Lee,‡[a] Hong-Jun Cho,[b] Seongsoo Kim,[a] Dong-Sik Shin *[c] and Sang-Myung Lee*[a]

Received 11th April 2017
Accepted 6th June 2017

DOI: 10.1039/c7ra04107a

rsc.li/rsc-advances

Polydopamine (PDA) is considered as a fluorescent molecule, however, the molecular structure and degree of polymerization that yield the most efficient fluorescence have yet to be identified. Here, we first present the fluorescence origin of polymerized dopamine derivatives (pDA) and their extraordinary behavior on the ultra-selective recognition of Fe^{2+} ions. Dopamine molecules are polymerized to 5,6-dihydroxyindole-rich pDA in basic conditions, followed by readily oxidizing to indole-5,6-quinone-rich pDA by dropping the pH to strongly acidic conditions. It was clearly demonstrated that oligomeric dopamine molecules were water-soluble with intense fluorescence (F-ODA, $n = 3$–4), while polymeric dopamine molecules were water-insoluble without fluorescence (PDA, $n > 5$). Also, F-ODA was dramatically selective to Fe^{2+} ions contradicting previous studies, and their unique binding mechanism was described through the redox potential analysis.

Introduction

With the rapid development of optical analysis, fluorescence-based detection and imaging techniques have been widely applied in the field of biotechnology. Many fluorescent probes featuring Stokes shifts have been studied, however, most of the commercially available fluorescent organic probes have limitations, such as high *in vitro* and *in vivo* toxicity, low quantum yields, and poor solubility and stability in water.[1] To overcome these problems, fluorescent probes based on biocompatible or bio-inspired materials have recently been developed showing good biocompatibility and biodegradability with high fluorescence and low toxicity.[2]

Dopamine, a member of the catecholamine family, is well known for its role in neurotransmission and hormone release control. Dopamine is converted into 5,6-dihydroxyindole through cyclization induced by oxidative nucleophilic reaction under weakly basic conditions, after which it is polymerized to polydopamine (PDA) through covalent bonding, hydrogen bonding, π–π interactions and so on.[3,4] Owing to its strong adhesive properties, PDA has been used as a surface coating to increase the stability or modify the surface of organic or inorganic materials.[4] Also, chelation of Fe^{3+} ions with dopamine or dopamine derivatives is a well-known coordination induced by the attraction between catechol groups and Fe^{3+} ions. Based on this coordination, PDA cellulose nanocrystals (PDA@CNC) or PDA montmorillonite (PDA@Clay) were used to detect pollutants including Fe^{3+} ions.[5,6] Moreover, nanoparticles consisting of PDA and Fe^{3+} ion complexes (PDA@Fe^{3+}) were used as agents for MRI, bioimaging, and drug delivery systems.[7–10] However, to the best of our knowledge, it is still unclear which structures of polymerized dopamine derivative (pDA) are mainly responsible for strong fluorescence. Bayindir *et al.* reported fluorescent PDA nanoparticles could be synthesized under basic conditions, however, they did not clearly present the origin of this fluorescence.[11] In contrast, Xu *et al.* asserted that PDA nanoparticles do not emit fluorescence, but serve as fluorescence quenchers for some fluorescent dyes.[12] This dispute is based on uncertainty over which molecular structures of PDA and which degrees of polymerization of dopamine are empirically effective for achieving fluorescence. Recently, Wu *et al.* and Tseng *et al.* reported that relatively low-molecular-weight polymers emit fluorescence.[1,13] However, their methods have some disadvantages regarding the requirement of several additional chemical processes to control the molecular weight of polymerized dopamine derivatives.

Ferrous (Fe^{2+}) and ferric ions (Fe^{3+}), which are abundant metal ions in the human body, play important roles in various biological processes such as electron transport, enzymatic reaction, oxygen delivery and composition for heme.[14,15]

[a]*Department of Chemical Engineering, Kangwon National University, Gangwon-do 24341, Republic of Korea. E-mail: sangmyung@kangwon.ac.kr*

[b]*School of Chemical and Biological Engineering, Seoul National University, Seoul 08826, Republic of Korea*

[c]*Department of Chemical and Biological Engineering, Sookmyung Women's University, Seoul 04310, Republic of Korea. E-mail: dshin@sm.ac.kr*

† Electronic supplementary information (ESI) available. See DOI: 10.1039/c7ra04107a

‡ These authors contributed equally to this work.

Disruption of iron equilibrium in cells results in various diseases such as cancer, hepatitis, Alzheimer disease and Parkinson's disease.[16] Especially, reactive oxygen species that have critical effects on cells could be formed by reaction between ferrous ions (Fe^{2+}) and hydrogen peroxide.[17] In spite of importance of Fe^{2+} ions, there are few sensing model due to its poor selectivity.[18–20]

Herein, we first identified the fluorescence origin of pDA and their extraordinary behaviour on the ultra-selective detection of Fe^{2+} ions. Dopamine molecules are polymerized to 5,6-dihydroxyindole-rich pDA in basic condition. By dropping pH to the strong acidic condition, 5,6-dihydroxyindole-rich pDA is readily oxidized to indole-5,6-quinone-rich pDA through the redox reaction with dissolved oxygen. We observed that oligomeric dopamine was water-soluble with intensive fluorescence (F-ODA, $n = 3$–4), meanwhile polymeric dopamine molecule was water-insoluble without fluorescence (PDA, $n > 5$). We also found that F-ODA was dramatically selective to Fe^{2+} ions, contradicting previous studies reporting that only Fe^{3+} ions interact with dopamine derivatives. Their unique binding mechanism was elucidated through the redox potential analysis.

Results and discussion

Synthetic mechanism of F-ODA

The overall isolation procedure and proposed structures of the polymerized dopamine derivatives in each step are presented in Scheme 1. Dopamine was polymerized by increasing pH of the dopamine dissolved in PBS buffer. The main polymerized products were 5,6-dihydroxyindole-rich compounds composed of various polymerized dopamine derivatives, including polymers and oligomers. As this product was acidified by adding HCl, the 5,6-dihydroxyindole-rich compound was oxidized to an indole-5,6-quinone-rich compound. Since the non-fluorescent PDA was precipitated, the fluorescent F-ODA supernatant containing indole-5,6-rich compounds could be well separated.

To prove this proposed mechanism, the structures were revealed by measuring optical properties in each step. First, we investigated the chemical structures of dopamine, the 5,6-dihydroxyindole rich compound, the indole-5,6-quinone-rich compound, and F-ODA *via* FT-IR spectroscopy (Fig. 1). The FT-

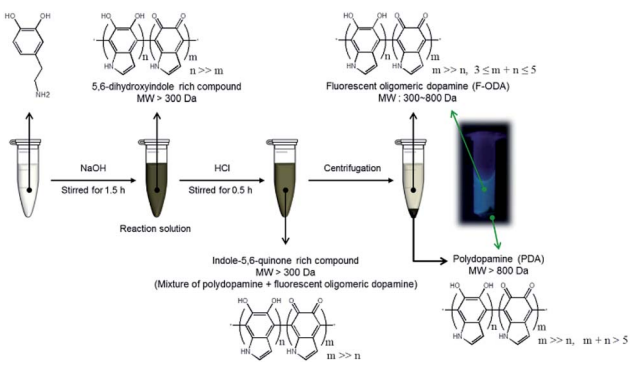

Scheme 1 Overall scheme for the polymerization of dopamine and proposed structures in each step.

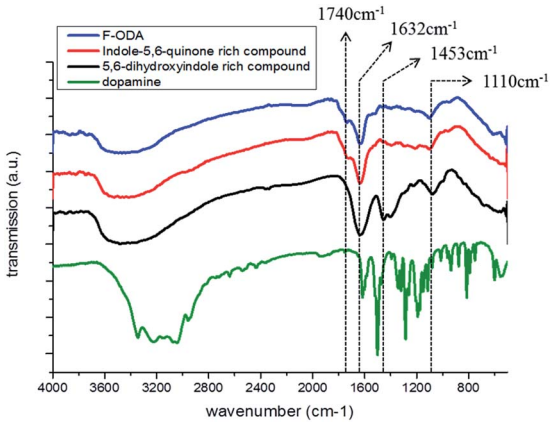

Fig. 1 FT-IR spectra of dopamine (green), 5,6-dihydroxyindole-rich compound in basic conditions (black), indole-5,6-quinone-rich compound in acidic conditions (red), and F-ODA (blue).

IR spectrum of dopamine exhibited five bands: stretching and bending vibrations of the amine group (3340 and 1618 cm^{-1}, respectively), the stretching vibration of the hydroxyl group of catechol (3320 cm^{-1}), and the stretching vibrations of C–H (3040 cm^{-1}) and C–C of the aromatic ring (1550 cm^{-1}).[21,22] After polymerization in basic condition (black line), three distinguishable bands appeared at 1632, 1453, and 1110 cm^{-1}, corresponding to the stretching vibrations of the aromatic ring, the specific structure of polyindole, and the C–O of the phenol group, respectively.[23,24] This finding suggested that the polymerized dopamine derivatives were mainly composed of 5,6-dihydroxyindole. However, acidification by HCl addition (red line) induced the structural transition of 5,6-dihydroxyindole to indole-5,6-quinone, which was identified by observing a new band at 1740 cm^{-1} corresponding to ketone and the weakening or disappearance of peaks at 1453 and 1110 cm^{-1} corresponding to 5,6-dihydroxyindole.[25] We also determined that the structure of F-ODA was mainly composed of indole-5,6-quinone on the basis of the similarity of the FT-IR spectrum of F-ODA (blue line) to that of the indole-5,6-quinone-rich compound (red line).

In addition to the FT-IR analysis, redox reaction analysis was performed. Fig. 2 presents a redox potential diagram indicating the expected half-reactions upon HCl addition to the basic reaction solution and the pH-dependent redox potentials.[26,27] These two half-reactions clearly indicate that the sudden pH drop can trigger the reduction of dissolved oxygen by supplying excess protons, leading to the spontaneous oxidation of 5,6-dihydroxyindole to indole-5,6-quinone. Since indole-5,6-quinone became more neutral than 5,6-dihydroxyindole, this oxidation can decrease the solubility of the indole-5,6-quinone-rich compound. As a result, the polymeric molecules of the indole-5,6-quinone-rich compounds were aggregated through the hydrophobic interaction, π–π interaction and hydrogen bonding, and then precipitated in aqueous solution while the oligomeric molecules remained in the supernatant.[4]

Meanwhile, the mass spectrum of F-ODA exhibited several peaks at m/z 445, 569, 656, 672, 719, and 861, corresponding to

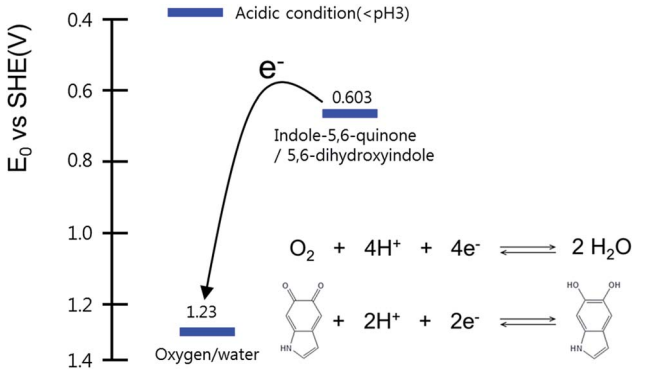

Fig. 2 Schematic reduction potential diagram of indole-5,6-quinone and oxygen indicating that the reduction of dissolved oxygen and the oxidation of 5,6-dihydroxyindole can be triggered by adding many protons.

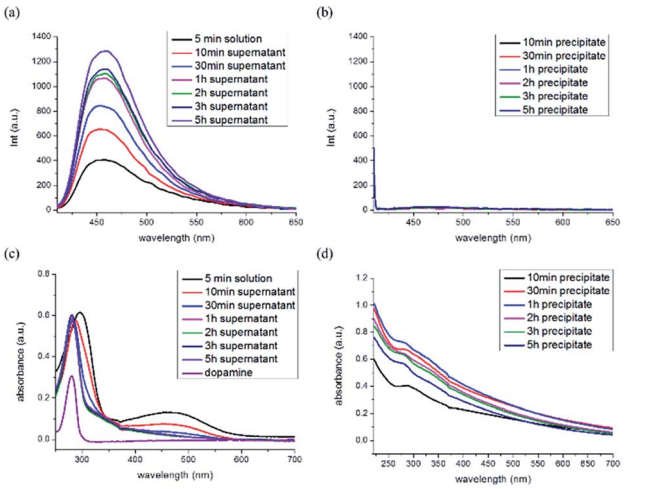

Fig. 3 Fluorescence spectra of the (a) supernatant and (b) precipitate and UV/Vis absorption spectra of the (c) supernatant and (d) precipitate as a function of reaction time (λ_{max} = 400 nm).

[m], [n + 2Na + 2K], [p + Na + K], [p + 2K], [p + 2Na + 2K], and [q + 2Na + 2K], respectively (Fig. S1a†). Fig. S1b† shows the expected chemical structures of m, n, p, and q, indicating that F-ODA has an oligomeric structure featuring 3–5 degrees of polymerization. Furthermore, from NMR analysis of F-ODA compared with pure dopamine, the chemical shift of aromatic protons disappeared and the shift of methylene groups migrated (Fig. S2†).[28,29] In addition, XPS analysis of F-ODA exhibited C 1s spectrum at 284.68 eV (C–C or C=C) (Fig. S3(a)†), N 1s spectrum at 399.38 eV (C–N–C or N–H) (Fig. S3(b)†) and O 1s spectrum at 532.28 eV (C=O and C–OH) (Fig. S3(c)†).[30] These data indicated that the dopamine polymerization reaction was successfully performed.

Optical property of F-ODA

We investigated the optical properties of the F-ODA supernatant and PDA precipitate under different reaction conditions by fluorescence and UV/Vis absorption spectroscopies, as shown in Fig. 3. The fluorescence of the F-ODA supernatant in 10 mM sodium hydroxide solution was found at 457 nm (λ_{ex} = 400 nm) and increased gradually while the PDA precipitate did not emit any fluorescence over time (Fig. 3(a) and (b)). In subsequent experiments, the reaction time was set to 1.5 h, which was considered sufficient to show high fluorescence intensity. The UV/Vis absorbance bands of the F-ODA supernatant were observed at 300 nm and 457 nm at the beginning of the polymerization reaction (Fig. 3(c)). As polymerization reaction time goes by, the absorbance bands observed at 300 nm was blue-shifted to 280 nm same as that of dopamine, and the band at 457 nm completely decreased within 30 min. The absorbance bands at 300 nm and 457 nm are those of dopaminechrome which is one of the intermediate molecules produced during the polymerization. Moreover, dopaminequinone molecules that are considered as an early form of dopaminechrome were not detected because their oxidation rate is too fast (395 nm).[31] Considering that the maximum absorbance wavelength (280 nm) is different from the excitation wavelength (400 nm), the findings also confirmed that F-ODA has various singlet states, as fluorescence can only occur when the excited electrons drop from the S1 level to the S0 level. The high energy at 280 nm might be capable of exciting the electrons to higher singlet states than S1, whereas the weaker energy at 400 nm is capable of excitation at most from S0 to S1. In the case of the PDA precipitate, a shoulder peak was observed at 280 nm, which is identical to the peak of F-ODA (Fig. 3(d)).

The effect of pH to initiate the polymerization was investigated by adding various concentrations of NaOH solution into the reaction mixture. The fluorescence intensity at 457 nm was highest when 4 mM NaOH was added (pH = 10.7) (Fig. S4†). Since more NaOH induced extensive polymerization, polymeric dopamine was dominant at higher pH resulting in low fluorescence. In the following experiments, the NaOH concentration was set to 4 mM to maximize the fluorescence intensity.

Next, the effect of HCl on the molecular structural change of the polymerized dopamine derivatives *via* redox reaction was investigated (Fig. S5(a)†). In the absence of HCl, the 5,6-dihydroxyindole-rich compound could not be separated into a precipitate and supernatant by centrifugation; thus, the fluorescence intensities were totally same before and after centrifugation (Fig. S5(b)†). On the other hand, the fluorescence intensity of the F-ODA supernatant obtained from the indole-5,6-quinone-rich compound by centrifugation was higher than that of the indole-5,6-quinone-rich compound (Fig. S5(c)†). This fluorescence increase is caused by the removal of PDA, which partially absorbs the incident light (400 nm) exciting F-ODA. With respect to this phenomenon, Fig. S6† supports our claim that 5,6-dihydroxyindole can be oxidized *via* the reduction of dissolved oxygen induced by the prompt addition of HCl. When HCl was added under deoxygenated conditions achieved by nitrogen purging, no precipitate was observed after centrifugation similarly to the result in the absence of HCl. This result strongly supports our hypothesis that the reduction of dissolved oxygen plays an important role in separating F-ODA. Based on optimized reaction conditions, we measured photoluminescence lifetime and

quantum yield of F-ODA. The F-ODA lifetime was shown as two types of decay: 1.75 ns (23.89%, short decay) and 5.05 ns (76.11%, long decay). From this result, the average lifetime was approximately 4.26 ns (Fig. S7(a)†). The F-ODA quantum yield was calculated 6.22% using eqn (1) compared with anthracene as a reference (Fig. S7(b)†).

$$Q = Q_R \left(\frac{m}{m_R}\right)\left(\frac{\eta^2}{\eta_R{}^2}\right) \quad (1)$$

Ultra-selective detection of Fe^{2+} ions

To investigate the fluorescence intensity changes of F-ODA depending on its chelation with various metal ions, we performed metal screening using F-ODA. When the acidic F-ODA solution was incubated with Ru^{3+}, Fe^{3+} and Fe^{2+}, the fluorescence prominently diminished among various metal ions (Fig. 4(a)). Based on the ratio of the initial to the final intensity at $\lambda_{max} = 457$ nm, Fe^{2+} quenched a fluorescence dramatically, decreasing the fluorescence intensity by 15-fold to the initial intensity (Fig. 4(b)). Fe^{3+} and Ru^{3+} are well-known chelate metal ions in the *ortho*-dihydroxyl group of catechol as well as fluorescence quenchers; thus, their quenching effects suggest that they are chelated with a few catechol groups of 5,6-dihydroxyindole of F-ODA.[32–34]

Since Fe^{2+} is not known to chelate with catechol, our discovery might be a surprising and inspiring result for further studies. Fig. S8† shows the redox half-reactions and the redox potentials associated with the half-reactions that could occur when adding Fe^{2+}.[26,27] As seen from the net reaction equation, the net redox potential is $E_0 = -0.167$ V under acidic conditions, thus the reaction between indole-5,6-quinone-rich F-ODA and Fe^{2+} is unfavorable under standard condition. However, the real potential difference E_h should consider the concentration of reactants, thus, we adopted the Nernst equation as shown in eqn (S1).† Before Fe^{2+} was added into the acidic F-ODA solution in the absence of Fe^{3+}, indole-5,6-quinone was dominant. In this condition, we can assume that the prompt addition of Fe^{2+} was enough to trigger an α-direction reaction. The reaction resulted in the increase of Fe^{3+} concentration leading to the α'-direction. However, Fe^{3+} was immediately chelated with reduced 5,6-dihydroxyindole and quenched the fluorescence (Fig. 5).

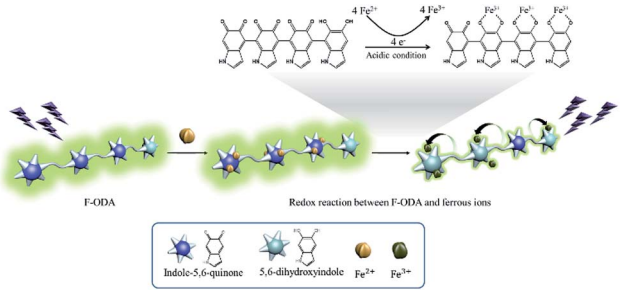

Fig. 5 Proposed mechanism for detection of ferrous ions *via* redox reaction between F-ODA and ferrous ions.

This result could be confirmed by monitoring the FT-IR spectra of F-ODA as well. Initially, the two bands at 1453 and 1110 cm^{-1} decreased upon the addition of HCl, corresponding to the stretching vibration of the specific structure of polyindole and the C–O of the phenol group respectively (Fig. 6, black line). Thereafter, the peaks were restored by the addition of Fe^{2+} ions (Fig. 6, red line). We conceived that it was due to a combination of two successive mechanisms: (1) reduction of the indole-5,6-quinone to catechol-structured 5,6-dihydroxyindole along with oxidation of Fe^{2+} to Fe^{3+} ions and (2) chelation of Fe^{3+} ion with reduced F-ODA. This hypothesis supported the result that Fe^{2+} ion quenched the fluorescence of the acidic F-ODA than Fe^{3+} ion even though Fe^{3+} is chelated with catechol groups directly. Additionally, SEM-EDS analysis was performed before and after incubating F-ODA with Fe^{2+} ions. From the SEM-EDS results, the synthesized polydopamine derivatives from supernatant and precipitate, respectively, showed very similar elemental analysis results (C: 30 wt%, N: 4 wt%, O: 61 wt%) (Fig. S9(a)

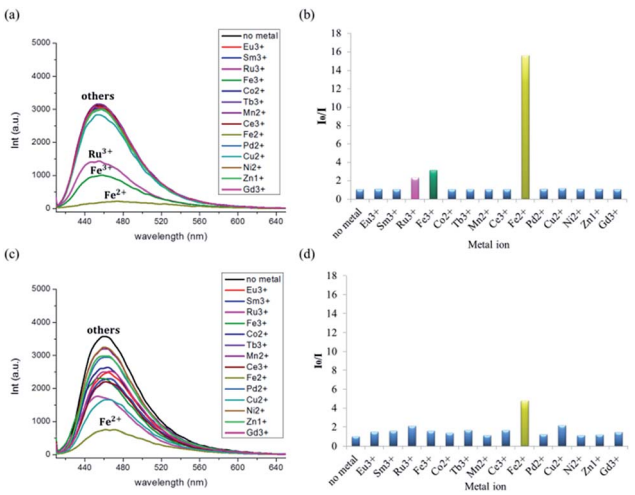

Fig. 4 (a) and (c) Fluorescence spectra and (b) and (d) fluorescence intensity ratios I_0/I of F-ODA upon addition of 1 mM of various metal ions at (a) and (b) acidic and (c) and (d) physiological pH.

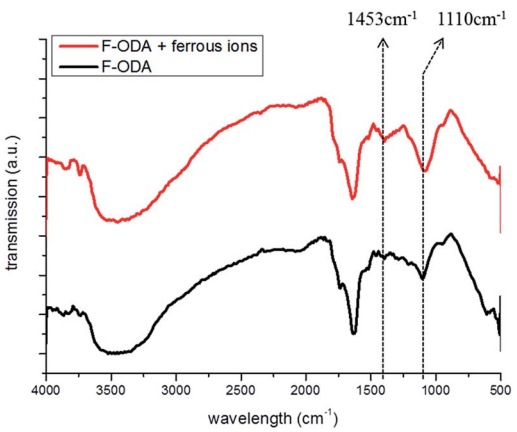

Fig. 6 FT-IR spectrum of F-ODA (black) and F-ODA + ferrous ions (red).

and (b)†). After incubating F-ODA with Fe^{2+} ions, we could confirm that Fe^{2+} ions were incorporated within F-ODA (Fig. S9(c)†).

We also confirmed that the fluorescence-quenching induced by Fe^{2+} decreased when the F-ODA solution reacted with Fe^{2+} after its pH was adjusted to 7.4, which was attributed to the lower reduction potential of indole-5,6-quinone at this pH compared with acidic conditions (Fig. 4(c) and (d)). This means that pH-dependent effect is also related to the formation of iron hydroxide at pH 7.4, which does not occur under acidic conditions.[35] Finally, we examined the dependence of the fluorescence intensity changes of F-ODA at pH 7.4 on the concentration of Fe^{2+} added. When the concentration of reacting Fe^{2+} increased from 2 μM to 1 mM, the fluorescence intensity of F-ODA at 457 nm decreased evidencing chelation between the oxidized Fe^{3+} and the reduced F-ODA (Fig. 7(a)). Fig. 7(b) shows that the fluorescence intensity ratio $(I_0 - I)/I_0$ at 457 nm is a function of Fe^{2+} concentration (I_0 and I represent the fluorescence intensities of F-ODA before and after Fe^{2+} addition, respectively). The inset graph of Fig. 7(b) indicates that the fluorescence intensity ratio $(I_0 - I)/I_0$ is linear in the range of 2–50 μM Fe^{2+}, showing that Fe^{2+} can be sensitively detected in this concentration range.

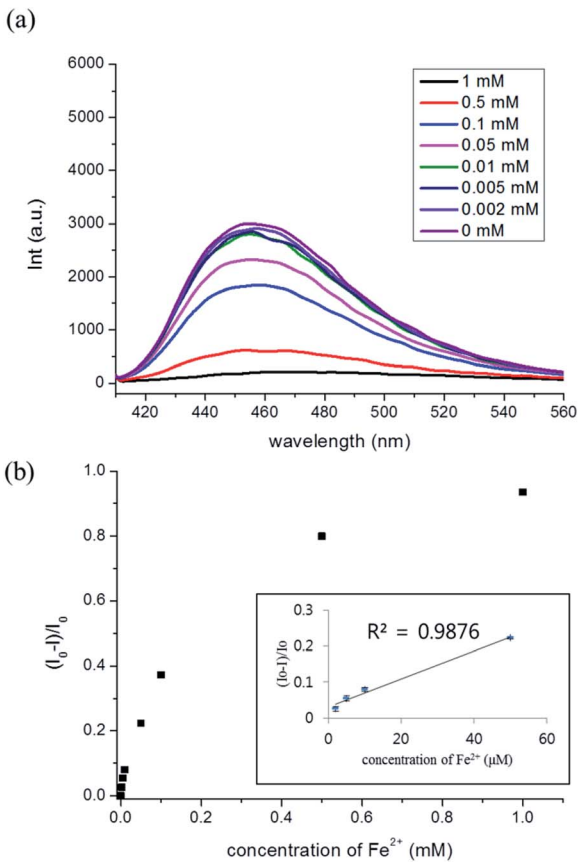

Fig. 7 (a) Fluorescence spectra and (b) fluorescence intensity ratios $(I_0 - I)/I_0$ of F-ODA upon the addition of different concentrations of Fe^{2+} ($n = 3$ in inset graph).

Experimental

Reagents and apparatus

The following were purchased from Sigma-Aldrich Co.: dopamine hydrochloride and the metals: europium(III) chloride, samarium(III) chloride hexahydrate, iron(III) chloride hexahydrate, ruthenium(III) chloride, cobalt(II) chloride hexahydrate, terbium(III) chloride hexahydrate, manganese(II) chloride tetrahydrate, cerium(III) chloride nonahydrate, iron(II) chloride tetrahydrate, zinc sulfate nonahydrate, and gadolinium(III) trifluoromethanesulfonate. Sodium hydroxide powder and hydrochloric acid were purchased from Daejung Co. Distilled water (Millipore) was used as a solvent for the metal ions. PBS buffer (pH 7.4, 2 mM) prepared in-house was used as a solvent for dopamine. UV/Vis absorption spectra and fluorescence emission spectra were collected using a UV/Vis spectrometer (OPTIZEN-α, Mecasys) and fluorescence spectrometer (FS-2, Scinco), respectively. FT-IR spectra were obtained using an FT-IR spectrometer (FTLA2000-104, ABB). Matrix-assisted laser desorption/ionization time-of-flight (MALDI-TOF) mass spectra of F-ODA were also recorded using a Voyager-DE STR workstation (Applied Biosystems).

Synthesis of fluorescent oligomeric dopamine

F-ODA was prepared by oxidative polymerization and separated from the precipitated PDA by centrifugation. In the first step, dopamine hydrochloride (0.378 mg, 1 mM final concentration) was dissolved in 1.8 mL of PBS buffer (pH 7.4, 2 mM), and oxidative polymerization was conducted in a 20 mL glass vial *via* magnetic stirring (200 rpm) at room temperature for 1.5 h with 0.2 mL of sodium hydroxide solution (4 mM final concentration). After stirring, 0.04 mL of hydrochloric acid (0.25 M) was added to the solution, and the solution was stirred for an additional 0.5 h to induce the reduction of oxygen and the oxidation of 5,6-dihydroxyindole. In the second step, the resulting solution was transferred to a 2 mL Eppendorf tube and separated by centrifugation (10 000 rpm) at room temperature for 10 min. The obtained supernatant was used to detect Fe^{2+} ions. The precipitate were fully re-dispersed with 2 mM PBS buffer solution (pH 7.4) to measure fluorescence intensity. The fluorescence intensities from the supernatant and the precipitate were measured at PMT 500 V using micro quartz cells.

Metal screening

Various metal ions were dissolved in 0.05 mL of DW to a concentration of 1 mM. Next, 0.2 mL of F-ODA solution and 0.05 mL of each metal solution were mixed in a 1.5 mL tube and reacted in a thermomixer at room temperature and 600 rpm for 30 min. In the case of measurement at physiological pH, the pH of the F-ODA solution was adjusted to physiological pH after the F-ODA had been separated.

Conclusions

In summary, we clearly demonstrated that the fluorescence of pDA originates from oligomeric dopamine, not from PDA. F-

ODA was separated from PDA by solubility difference induced by structural change from 5,6-dihydroxyindole-rich pDA to indole-5,6-quinone-rich pDA. In addition, fluorescence of F-ODA was dramatically quenched by only Fe^{2+} ions based on their unique redox mechanism. Since this ultra-selective recognition of Fe^{2+} contradicts previous reports insisting that only Fe^{3+} ions interact with dopamine derivatives, our discovery must be an outstanding and inspiring result for the further studies.

Acknowledgements

This work was supported by the Ministry of Science, ICT & Future Planning and National Research Foundation of Korea through Basic Science Research Program (NRF-2014R1A1A1006711 and NRF-2015R1D1A1A01059367), the Ministry of Trade, Industry & Energy (MOTIE), Korea Institute for Advancement of Technology (KIAT) through the Encouragement Program for The Industries of Economic Cooperation Region (R0004027) and Kangwon National University through 2015 Research Grant (No. 520150081).

Notes and references

1 B. Xiong, Y. Chen, Y. Shu, B. Shen, H. N. Chan, Y. Chen, J. Zhou and H. Wu, *Chem. Commun.*, 2014, **50**, 13578–13580.
2 X. Feng, L. Liu, S. Wang and D. Zhu, *Chem. Soc. Rev.*, 2010, **39**, 2411–2419.
3 J. Yang, M. Cohen Stuart and M. Kamperman, *Chem. Soc. Rev.*, 2014, **43**, 8271–8298.
4 Y. Liu, K. Ai and L. Lu, *Chem. Rev.*, 2014, **114**, 5057–5115.
5 Y. Han, X. Wu, X. Zhang, Z. Zhou and C. Lu, *ACS Sustainable Chem. Eng.*, 2016, **4**, 5667–5673.
6 S. Huang, L. Yang, M. Liu, S. L. Phua, W. A. Yee, W. Liu, R. Zhou and X. Lu, *Langmuir*, 2013, **29**, 1238–1244.
7 K. Y. Ju, J. W. Lee, G. H. Im, S. H. Lee, J. Pyo, S. B. Park, J. H. Lee and J. K. Lee, *Biomacromolecules*, 2014, **14**, 3491–3497.
8 K. Xin, M. Li, D. Lu, X. Meng, J. Deng, D. Kong, D. Ding, Z. Wang and Y. Zhao, *ACS Appl. Mater. Interfaces*, 2017, **9**, 80–91.
9 X. Zheng, J. Zhang, J. Wang, X. Qi, J. M. Rosenholm and K. Cai, *J. Phys. Chem. C*, 2015, **119**, 24512–24521.
10 B. Xiong, Y. Chen, Y. Shu, B. Shen, H. N. Chan, Y. Chen, J. Zhou and H. Wu, *Chem. Commun.*, 2014, **50**, 13578–13580.
11 A. Yildirim and M. Bayindir, *Anal. Chem.*, 2014, **86**, 5508–5512.
12 W. Qiang, W. Li, X. Li, X. Chen and D. Xu, *Chem. Sci.*, 2014, **5**, 3018–3024.
13 J.-H. Lin, C.-J. Yu, Y.-C. Yang and W.-L. Tseng, *Phys. Chem. Chem. Phys.*, 2015, **17**, 15124–15130.
14 P. Aisen, C. Enns and M. Wessling-Resnick, *Int. J. Biochem. Cell Biol.*, 2001, **33**, 940–959.
15 C.-D. Kaplan and J. Kaplan, *Chem. Rev.*, 2009, **109**, 4536–4552.
16 W. Xuan, R. Pan, Y. Wei, Y. Cao, H. Li, F.-S. Liang, K.-J. Liu and W. Wang, *Bioconjugate Chem.*, 2016, **27**, 302–308.
17 S. Maiti, Z. Aydin, Y. Zhang and M. Guo, *Dalton Trans.*, 2015, **44**, 8942–8949.
18 B.-P. Esposito, S. Epsztejn, W. Breuer and Z.-I. Cabantchik, *Anal. Biochem.*, 2002, **304**, 1–18.
19 J.-L. Chen, S.-J. Zhuo, Y.-Q. Wu, F. Fang, L. Li and C. Q. Zhu, *Spectrochim. Acta, Part A*, 2006, **63**, 438–443.
20 T. Hirayama, K. Okuda and H. Nagasawa, *Chem. Sci.*, 2013, **4**, 1250–1256.
21 Y. Ma, H. Niu, X. Zhang and Y. Cai, *Analyst*, 2011, **136**, 4192–4196.
22 S. Xiong, Y. Wang, J. Yu, L. Chen, J. Zhu and Z. Hu, *J. Mater. Chem. A*, 2014, **2**, 7578–7587.
23 C. Zhijiang and H. Chengwei, *J. Power Sources*, 2011, **196**, 10731–10736.
24 A. Banerjee, S. Supakar and R. Banerjee, *PLoS One*, 2014, **9**, 1–7.
25 S. Bose, S. Maji and P. Chakraborty, *AAPS PharmSciTech*, 2013, **2**, 72–74.
26 M. Amiri, E. Amali and A. Nematollahzadeh, *Sens. Actuators, B*, 2015, **216**, 551–557.
27 W. M. Haynes, *CRC Handbook of Chemistry and Physics*, CRC Press, Boca Raton, FL, 93rd edn, 2012.
28 M. Demura, T. Yoshida, T. Hirokawa, Y. Kumaki, T. Aizawa, K. Mitta, I. Bitter and K. Toth, *Bioorg. Med. Chem. Lett.*, 2005, **15**, 1367–1370.
29 M. Bisaglia, S. Mammi and L. Bubacco, *J. Biol. Chem.*, 2007, **282**, 15597–15605.
30 K. Qu, J. Wang, J. Ren and X. Qu, *Chem.–Eur. J.*, 2013, **19**, 7243–7249.
31 M. Bisaglia, S. Mammi and L. Bubacco, *J. Biol. Chem.*, 2007, **282**, 15597–15605.
32 D. J. Phillips, G.-L. Davies and M. I. Gibson, *J. Mater. Chem. B*, 2015, **3**, 270–275.
33 R. Yamahara, S. Ogo, H. Masuda and Y. Watanabe, *J. Inorg. Biochem.*, 2002, **88**, 284–294.
34 F. Liu, X. He, J. Zhang, H. Chen, H. Zhang and Z. Wang, *J. Mater. Chem. B*, 2015, **3**, 6731–6739.
35 V. Bonnefoy and D. S. Holmes, *Environ. Microbiol.*, 2012, **14**, 1597–1611.